IEEE Access
Multidisciplinary | Rapid Review | Open Access Journal

Received August 16, 2020, accepted September 21, 2020, date of publication September 24, 2020, date of current version October 7, 2020.

Digital Object Identifier 10.1109/ACCESS.2020.3026492

Control Methods for Standalone and Grid Connected Micro-Hydro Power Plants With Synthetic Inertia Frequency Support: A Comprehensive Review

IRFAN SAMI[1], NASIM ULLAH[2], S. M. MUYEEN[3], (Senior Member, IEEE), KUAANAN TECHATO[4,5], MD. SHAHARIAR CHOWDHURY[5], AND JONG-SUK RO[1]

[1]School of Electrical and Electronics Engineering, Chung-Ang University, Seoul 06974, South Korea
[2]Department of Electrical Engineering, College of Engineering, Taif University, Ta'if 21974, Saudi Arabia
[3]School of Electrical Engineering, Computing and Mathematical Sciences, Curtin University, Perth, WA 6102, Australia
[4]Environmental Assessment and Technology for Hazardous Waste Management Research Center, Faculty of Environmental Management, Prince of Songkla University, Songkhla 90110, Thailand
[5]Faculty of Environmental Management, Prince of Songkla University, Songkhla 90110, Thailand

Corresponding author: Jong-Suk Ro (jongsukro@gmail.com)

This work was supported in part by the Basic Science Research Program through the National Research Foundation of Korea funded by the Ministry of Education under Grant 2016R1D1A1B01008058, and in part by the Human Resources Development of the Korea Institute of Energy Technology Evaluation and Planning (KETEP) grant funded by the Korea Government, Ministry of Trade, Industry and Energy (MOTIE), under Grant 20204030200090.

ABSTRACT The penetration of renewable energy sources on a large scale in conventional electric networks increases exponentially for environmental preservation. However, the increase in RESs leads to some technical problems that include (a) fluctuations in power production, (b) less or no generation units for power balancing, (c) reduced inertia due to RESs decoupling from the conventional grid using converters. Micro-hydro power plants (MHPPs) are emerging as a mature balancing technology and a great alternative to large hydropower plants as they encounter population displacement and many environmental problems. Modern pump storage MHPPs uses a power converter between the grid and machine to control the consumption of power during pumping mode. This power electronic interface loses the ability of the rotating mass of the machine to contribute to the grid inertia by making it independent of the grid frequency. This problem is solved through the control of power converters in such a way that the inertia effect is synthesized termed as synthetic inertia. MHPPs can also be operated in a standalone mode where they are not connected to the grid. This paper reviews control schemes applied in literature for the frequency, voltage, and inertia control, in both the grid-connected and standalone modes. This study starts with the standalone MHPPs, covering the literature review and control structure for voltage and frequency control of standalone MHPPs. Then it presents a detailed operation, control principle, synthetic inertia concepts, and architecture of grid-connected MHPPs. The mathematical formulation of the grid, permanent magnet synchronous generator, synthetic inertia inclusion, and control structures, including direct torque control, virtual synchronous machine, and model predictive control, is also presented. Finally, the paper presents the concluding remarks with the comparative analysis of various control structures to include synthetic inertia, its suitability, and future scope for MHPPs.

INDEX TERMS Frequency support, micro hydro power plants, standalone micro hydro plants, synthetic inertia.

NOMENCLATURE

S_g	apparent power nominal value
$V^*_{s,dq}$	PMSG stator dq voltages
P_G	Generator active power
i_{ds}, i_{qs}	Stator (dq) currents
$L_{m,dq}$	magnetizing inductance in dq windings
V_{DC}	DC Link Voltage
ω_m	Rotor angular speed

The associate editor coordinating the review of this manuscript and approving it for publication was Huanqing Wang.

v_{ds}, v_{qs}	Stator (dq) voltages
T_l	Load torque
Q_g	grid reactive power
$i_{g,abc}$	grid current
$L_{m,eq}$	equivalent inductance between generator and converter
i_{dc}	DC link current
$e_{g,dq}$	grid d voltage
$v_{g,dq}$	generator dq voltage
C_{dc}	DC link capacitor capacitance
P_r^*	virtual mechanical input power
f_{vsm}	VSM frequency
$\Delta f\,vsm$	deviation in VSM frequency
ω_b	base speed
v_{PLL}	filtered voltage in PLL
$v_{T,dq}^*$	converter reference dq voltages
$v_{T,dq}$	converter dq voltages
q_{hr}	head race tunnel flow
P_D	power delivered to ballast resistance
f_g	grid frequency
f_g	grid frequency
$f_{g,ref}$	reference grid frequency
T_m	Aerodynamic torque
$L_{s,dq}$	Stator dq inductance
R_s	Stator resistance
$e_{g,abc}$	grid voltage
λ_{sd}, λ_{sq}	stator (dq) fluxes
T_{em}	Electromagnetic torque
J	Moment of inertia
P_g	grid active power
P_g^*	the reference grid power
$R_{g,eq}$	equivalent resistance
$L_{g,eq}$	equivalent inductance between grid and converter
i_l	load current
$i_{g,dq}$	grid dq current
f_g	grid frequency
$i_{r,dq}$	damping winding current
P_d	droop power
f_{vsm}^*	reference VSM frequency
$\delta\theta_{vsm}$	deviation in VSM angle
f_g	grid frequecy
$f_{LP,PLL}$	low pass filter frequency
θ_{PLL}	instantaneous actual phase angle
P_l	load power
q	water flow
P_m	Turbine power

I. INTRODUCTION

The penetration of renewable energy sources (RESs) based distributed generation (DG) units is increasing rapidly. For example, Japan plans to integrate a 14.3 GW photovoltaic (PV) electrical energy to the conventional grid in 2020, raising it to 53GW by 2030 [1]. The power grid is undergoing a massive transformation from centralized power production to more flexible, and a new power system is known as "Smart grid (SG)" shown in Fig. 1. Renewable energy utilization in SG increases and supports the grid by improving power quality, reliability, and cost reduction [2]. In such modern power systems, where the RESs has high penetration, they have no or negligible inertia and damping properties. According to [3], it is predicted that the total decrease in inertia 70% in the UK between 2013/14 and 2033/34. This will cause the increase of the rate of change of frequency (ROCOF) of the power grid leading to the load shedding controller activation at a small imbalance in grid quantities. The author in [4] evaluated the ROCOF using several RESs penetration levels with a Synchronous Generator (SG) acting as MHPPs and founds that the ROCOF increases directly with the increase in the number of RESs as shown in Fig. 2. On the other hand, the conventional grid system uses bulky synchronous machines, which are the primary source of inertia. These synchronous machines play a significant role in the stability of the grid through its inherent rotor inertia and damping property due to electrical and friction losses in damper, stator, and field windings. As the RESs penetration increases, the problem of grid stability due to low inertia and damping effect also increases. Other issues like a rise in voltage due to reverse power flow from PV generating units [5], surplus power supply in the grid due to DGs operating at full capacity, frequency regulation degradation [6], and fluctuations in electric power due to the RESs variable operations. Such types of problems can be mitigated through the introduction of inertia in the grid system. In this new power system, energy storage plays a vital role in ensuring a constant electric

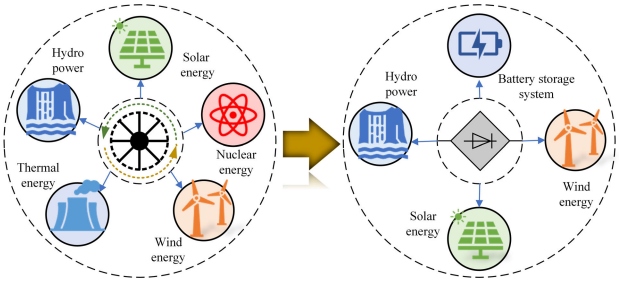

FIGURE 1. Evolution of REGs based modern power system.

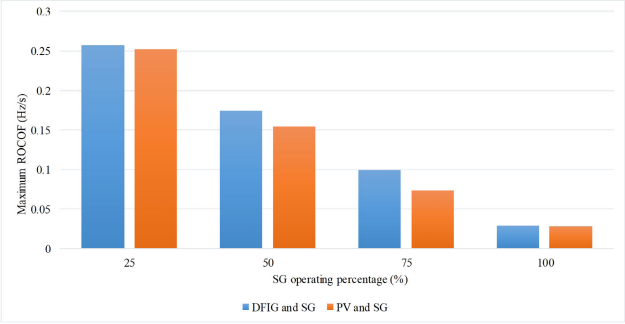

FIGURE 2. ROCOF relation with RESs installing capacity [4].

power [7]. 99% of the electricity storage all around the world constitutes hydropower, thus playing a significant role in the ensured and reliable power supply. The pumped storage micro hydroelectricity plants (PS-MHPPs) works in two modes: (a) generation: when there is a shortage of power in the grid, then the water in the reservoir is used to generate electricity (b) pumping: when there is a surplus of power in the grid, then this surplus power is used to pump water back to the reservoir. These PS-MHPPs are less flexible to the rapid variations and fluctuations in power production and need a modern control scheme to ensure constant power production. To solve this problem, the power electronic converter comes into play, and the machine is then decoupled from the conventional grid using adjustable speed units to control in a much efficient way. The high precise power production control of machines in PS-MHPPs using power converters contributes to the frequency stability of the power grid [8]. However, the inertia contribution of the PS-MHPPs is lowered due to the introduction of power converters.

In recent years, many solutions have been proposed to cope with the inertia contribution problem for converter controlled MHPPs. The most well-known techniques are classical torque control and virtual synchronous machine (VSM). This paper presents a comprehensive review of the various frequency and inertia control methodologies and their operation covered in the literature. Mathematical formulations of the components and control in MHPPs are presented. Detailed insight of the inertia emulation for the direct torque control, VSM based control, PD and PID based droop control, and Model Predictive torque control is presented in this paper. Apart from grid-connected MHPPs, a detailed literature review of standalone MHPPs (SMHPPs) with its control structure is also presented in this paper. Moreover, the paper is organized as follow: Section II describes the literature review and control structure for SMHPPs. The architecture of the grid-connected MHPSs is presented in section III. This section also outlines various variable speed MHPPs topologies, a complete description of MHPP architecture, power system stability concepts, and inertia concepts. The mathematical modeling of SM and grid within an MHPP is presented in section 4. Section 5 reviews the inertia emulation based control schemes with its mathematical modeling for grid-connected MHPPs. Finally, the article is concluded in section V with future recommendations.

II. VOLTAGE AND FREQUENCY CONTROL OF STANDALONE MHPP

The SG used in standalone MHPP (SMHHP) is subjected to voltage and frequency variations due to continually varying load, resulting in excess heat and mechanical vibrations in SG [10]. The SG generator thus needs a control system to regulate the perturbations on the generator side, referred to as electrical control, turbine side referred to as mechanical control, or on both sides called electromechanical control. In turbine side control or mechanical control, the speed of water is regulated using an inlet valve to control the speed of water to maintain the constant frequency and voltage of the SMHHP [11]. Due to the high cost of the hydraulic governor (HG), HG is not a preferable option to maintain the frequency and voltage of a standalone MHPP (SMHHP). An electronic load controller (ELC) is considered as an alternative to the high-cost HGs. In the generator side control, dummy resistors known as dump load are employed to regulate the voltage and frequency during load variation. This dump load modifies the amount of power by absorbing the surplus active power to the dissipation circuit, thus keeping a constant frequency by minimizing the difference between the generated power and consumed power. A significant portion of the power was dissipated as heat in earlier ELCs connected to a resistive load. But with the modern control topologies, the surplus power is efficiently used. The various types of control schemes implemented in the literature [10] are shown in Fig. 3. This section will review various ELC schemes for SMHHP frequency and voltage regulation.

An ELC based on the power relay approach was proposed by Woodward *et al.* [12] in 1980 for voltage and frequency regulation. In 1984, Kormilo *et al.* [13] utilized power electronics switches instead of relays to smoothen the frequency and voltage regulation. Bonert, *et al.* change the configuration of the electronic topology to minimize the line distortion in SHMPP [14]. With the development of power electronics, new topologies were introduced for SMHHP based ELC system, e.g., TRIAC based regulators [15]–[22], Rectifier control based Silicon controlled Rectifier (SCR) [14], [23]–[25], and insulated gate bipolar resistor (IGBT) based uncontrolled rectifier [26]. Also IGBTs with different configurations based on number of legs were also introduced for MHPP based ELCs e.g. 2 leg IGBT converter [27], [28], 3 leg IGBT converter in [29], 4 leg IGBT converter in [30], [31] and 6 leg IGBT converter was proposed in [32]. Self-excited induction generators (SEIG) were initially employed to their robustness, reliability, and cost-effectiveness. Many control schemes were presented to regulate the frequency and voltage of SEIG; for example, an analog control scheme was proposed in [12], digital signal processor (DSP) based ELCs in [33], [34], the current control scheme in [15], a feedforward control scheme for ELC in [21], [24], [35], and P, PI, and PID based control schemes in [36]–[40]. For MHPPs using asynchronous generators, a PI-based frequency and voltage control technique is proposed in [30], [31], [41], PI-based power control technique is proposed in [29], [32], deadbeat control schemes in [42], PLL based integrated ELC in [43]–[45] and optimization-based control methods in [46]–[48]. Control schemes for SG were also proposed in the literature. The author in [49]–[51] proposed P and PI-based control schemes, fuzzy logic based power-sharing scheme for ELC controlled SG [52], and a PLC based ELC was proposed in [53].

A. CONTROL STRUCTURE OF SMHPP

The ELC works on the principle of active power balancing to control the frequency of the SMHPP. The power generated

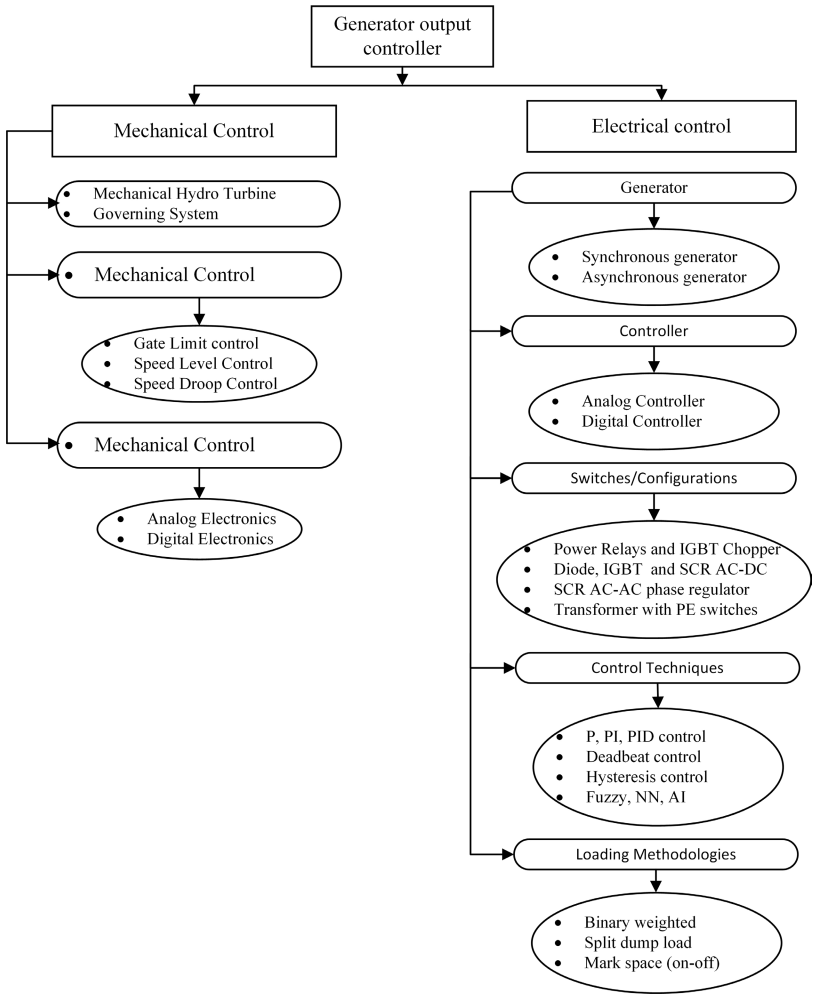

FIGURE 3. Control schemes for SMHHP.

is delivered to the load, whereas the access power is diverted to ballast resistive load. The operational diagram of the ELC based SMHPP control is shown in Fig. 4 Mathematically, this relation can be expressed as:

$$P_G = P_D + P_l \tag{1}$$

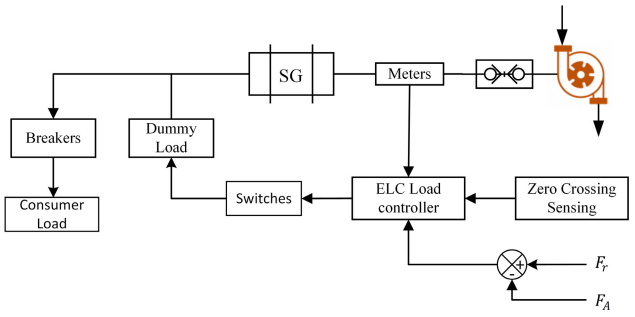

FIGURE 4. SMHHP operation.

The frequency control is performed by comparing the actual frequency with the reference frequency. An error between the actual frequency and reference frequency is generated, and then a controller (PI) is used to generate the firing angle. This firing angle decides the amount of power that should be dissipated through the dummy load. The firing angle can be expressed as:

$$\begin{aligned} \alpha &= K_p \Delta f + K_i \int \Delta f dt \\ \Delta f &= F_r - F_A \end{aligned} \tag{2}$$

where F_r and F_A are the reference frequency and actual frequency of the system. The per phase resistance value and power consumption of dump load that is considered equal to or slightly greater than the plant rated capacity are given as follow:

$$\begin{aligned} R &= \left. \frac{3V_s^2}{K \times P_G} \right|_{\alpha=0} \\ P_D &= \frac{V_s^2}{R} \left\{ \frac{1}{\pi} \left[(\pi - \alpha) + \frac{\sin 2\alpha}{2} \right] \right\} \end{aligned} \tag{3}$$

B. FUZZY BASED ELC CONTROL SYSTEM

The structure of the fuzzy-based ELC control presented in this section is based on the system proposed in [54] and shown

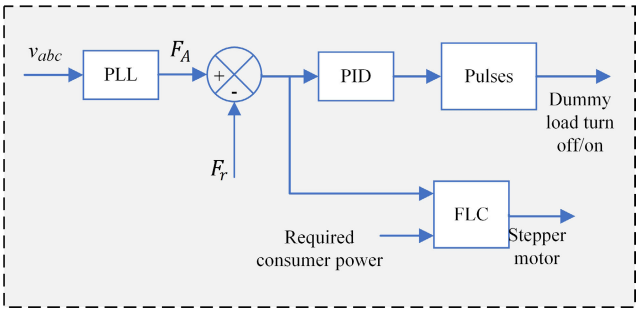

FIGURE 5. ELC using fuzzy logic control.

in Fig. 5. In this control system, the dummy load is controlled using pulses generated through the PI controller. The input to the PI is the deviation between the reference frequency and measured frequency. The fuzzy logic controller (FLC) controls the flow of water according to consumer power. If the required power is high, the FLC increases the water flow. The frequency is also controlled in the same way. If the generator frequency increase from the reference frequency, the dc motor is rotated to regulate the generator frequency by decreasing the water flow. In the case of a small deviation, the dummy load is switched on and off to regulate the frequency.

III. GRID-CONNECTED HYDRO POWER PLANTS ARCHITECTURE, FUNDAMENTALS, AND CONCEPTS

This section presents the architecture and the various typologies used in MHPPs. The basic concepts related to the penetration of power generated through MHPPs to the conventional grid are also explained in this section.

A. VARIABLE SPEED MHPPs TOPOLOGIES

The variable-speed operation of MHPPs is necessary for smooth power flow as fixed speed turbine leads to unstable operation in varying head reservoirs. For this purpose, variable speed turbines (VST) proves to be the right choice as the VSTs have much better efficiency with the capability of continuous and smooth operation [55]. The uninterrupted power supply can be made possible using the variable speed turbines with the inclusion of power electronics [56]. The output power of MHPP is directly proportional to the variation in the flow of water, thus increasing the chances of output power unbalance. A control system is necessary to control the power imbalance for stable and smooth operation at the consumer end [57]. The load and power balance can be achieved using pumped-storage MHPPs, that operates in two modes: (1) Generating mode and (2) Pumping mode. During peak hours or grid failure scenarios, the generating mode is active, maintaining uninterrupted power supply to the end load. Conversely, during the off-peak periods, the excess power in the pumped storage plant is used to pump the water from a low-level reservoir to the upper reservoir [58].

A grid-connected MHPP needs electric converters for its variable speed operation. There are two major topologies of MHPP that uses back to back converters for the grid-connected operation: Converter fed synchronous machine (CFSM) and doubly fed induction machine (DFIM). The CFMS is directly connected to the grid system using power electronic converters. In contrast, in the case of DFIM, the stator is directly connected to the grid while the rotor is connected to the grid through converters [59], as shown in Fig. 6. The main advantage of the DFIM topology is the variable speed operation achieved by applying low-frequency varying currents on its rotor; thus, the pumping power and the speed can be controlled using AC excitation [60]. The DFIM topology has an advantage of low rating converters utilization, as they need a converter to be rated as 30% of the machine rating. However, the complex rotor structure of DFIM topologies limits the rotor speed, thus making it unsuitable at high headed locations [61]. Conversely, the CFSM needs a converter rating the same as the machine, as the converters are subjected to the full power of the machine. The decoupled structure of the CFSM topology, less complicated structure, black start, option to bypass converters, and high starting torque of CFSM makes it more efficient than DFIM topology [61]. Comparative analysis of both the machines shows that the DFIM efficiency (98.3%) is

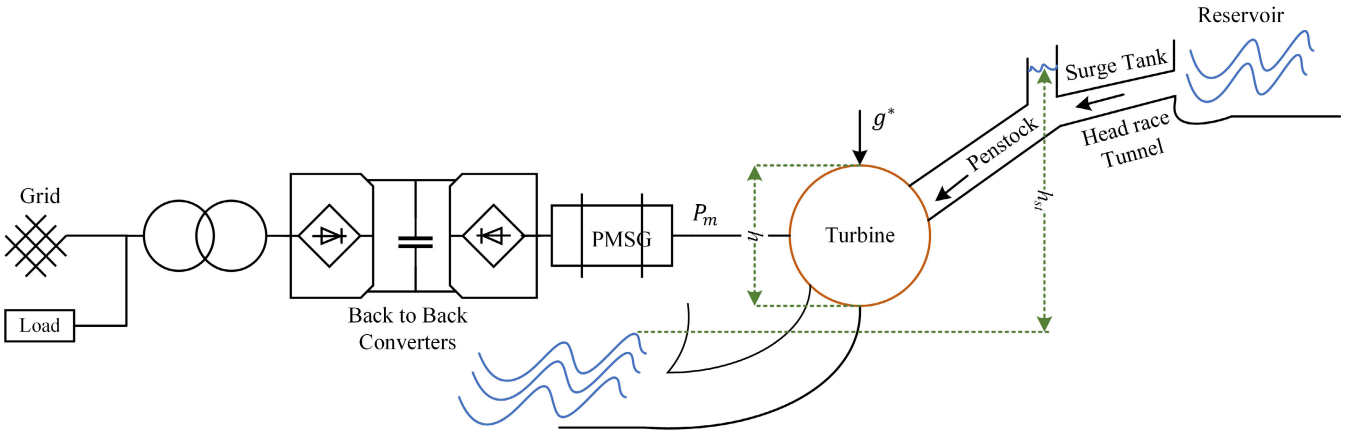

FIGURE 6. MHPP Layout.

less than CFSM (98.8%); however, for the overall topology, the converters affect the efficiency of CFSM, bringing it to 97.3% due to the losses in converters while the DFIM efficiency is lowered to 97.9% [62]. Other various topologies that are used for MHPPs are shown in Fig. 7.

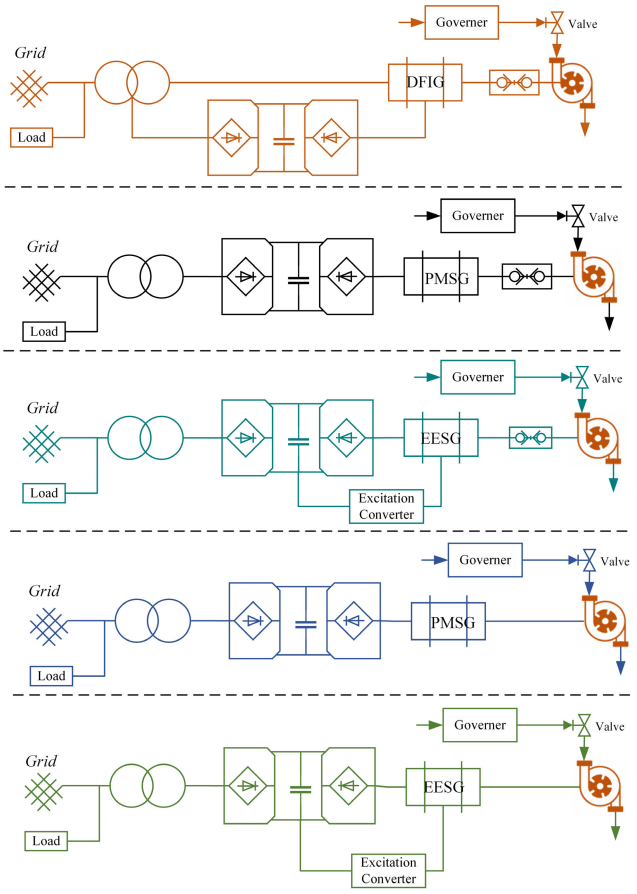

FIGURE 7. MHPPs topologies.

B. MHPP SYSTEM DESCRIPTION

A grid-connected MHPP, the hydraulic system, is presented in Fig. 6. The transformer separates the grid from MHPP, whereas the MHPP consists of an SM and back to back converters, used to integrate the power from SM into the grid. The SM is run by a turbine that transforms the kinetic energy of the water flowing from a reservoir through the penstock. The control topology of SM consists of a governor and an automated voltage regulator (AVR). There is two control mechanism to control grid-connected SGs: (1) control of the active power through the control of water flow into the turbine and (2) control of the reactive power flow from SG using AVR, that regulates the rotor excitation through the regulation of field current. The AVR works as an outer loop controller that aims to keep a constant stator terminal voltage. This controller takes the terminal voltage of the stator and uses a controller to generate a reference field current. The AVR excitation system sometimes uses a power system stabilizer to improve the power stability of the system by providing damping in the power system oscillation [64]. If the active and reactive power can be controller separately, then there is no need for a power stabilizer. Generally, the turbine and governor are modeled in terms of state-space equations. The input to the governor is the deviation in the nominal frequency/speed, and the output is the desired opening of the gates. The output of the gate governor act as input to the turbine, which generates mechanical power based according to the gate opening. The SM is then connected to the grid through converters. The modular multi-level converter (MMC) topology is nowadays widely accepted for high power conversion. A series of power cells or power semiconductors are needed for voltage above 3.3 kVLL for higher power levels [65], [66].

Two back to back converters are connected for stable operation of grid-connected MHPPs where one is termed as grid side converter (GSC) while the other connected to SM is termed as machine side converter (MSC). The DC link voltage is chosen as twice the peak of the phase voltage. The line between the SM and the grid has impedance classified as (a) impedance between transformer and GSC, (2) GSC impedance, and (3) machine impedance in series with the MSC impedance [2]. SG is the significant component of the grid-connected MHPPs for converting mechanical energy into electrical energy. They are used on a large scale to produce power from steam turbines, hydro turbines, or combustion engines [67]. The most prominent features of SM as compared to other machines are: (1) its output power may be in proportion to grid frequency, (2) the terminal voltage of SM can be accurately controlled through an excitation system, (3) it has high short circuit current, and (4) it has short term frequency regulation from inertia response [68]. A detailed comparison of the DFIM versus SM is given in table 1 portraying the premium feature of both the topologies in MHPPs.

C. POWER SYSTEM STABILITY AND SYNTHETIC INERTIA

A power system is said to be stable if it is capable of regaining itself after the occurrence of any disturbance. This stability can be categorized into three subcategories: (1) Voltage stability, (2) Rotor angle stability, and (3) frequency stability. IEEE power system engineering committee defines the voltage stability as: ''Voltage stability is the system able to maintain voltage such that the power and voltage can be controlled and load power increases with the increase in load admittance'' [69]. The rotor angle stability is the ability of the system to be synchronized during a disturbance. The frequency stability is related to balancing of active power and its ability to maintain constant frequency when there is an imbalance between load and generation [70]. The response of frequency for English and wales with the operating limits is shown in Fig. 8 [71]. It can be seen that; the regular operating frequency of the system is close to 50 Hz. However, the demand-generation imbalance condition, a decline in the system frequency, starts. The rate of decline of the frequency depends on the amount of unbalanced power and the total system inertia. This ROCOF is expressed by the swing

TABLE 1. Performance analysis of DFIM and SMC in terms of various dynamics.

Features	DFIM	SM
Excitation	Excitation 3-phase AC excitation	Low DC field voltage and current in the rotor circuit
Speed	the synchronous speed with a wide range of operating speeds	can operate at: Synchronous speed Sub synchronous speed Super synchronous speed
Starting	Requires damper winding for start-up	Self-starting
Power factor	Can be controlled using D.C excitation	Requires PE converters for power factor control
Efficiency	• 98.3% for standalone • 97.9 % for converter connected	• 97.8 % for standalone • 97.3 % for converter connected
Power electronics requirements and Cost	• Power electronics converters are must for operation • Operated at partial rated converters • Rating is dependent on the slip • Low installation cost due to partial rated converters	• Can be operated without power electronics converters • Converter rating same as machine rating High installation cost due to full rated converters
Power generation	Stator and rotor both contribute to power generation	Only stator contributes to power generation
Fault tolerance	• Less control capability under grid failures due to dynamic increase in voltage • Possess high reactive power oscillations and low active power oscillations during grid failures • Faster response time to active and reactive power demands • High stability during both high and low speeds	• Drooped voltage when grid fails • Need disconnection to operate during grid failure • Less power oscillations
Operating range	Operates at rated power	Can be operated on partial loads
Power quality	• High power producing capability compared to SM • Decoupled Active and Reactive power	Operates under all any power factor making it viable to improve power factor

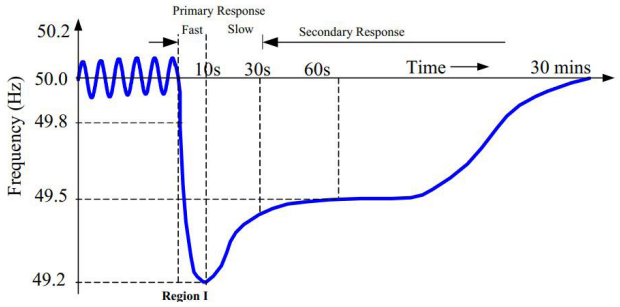

FIGURE 8. System frequency response time frames [3].

equation [9], [64], [72] given as:

$$P_g - P_l = \frac{d\,(E_k)}{dt} = \frac{d\left(\frac{1}{2}Jf_g^2\right)}{dt} \tag{4}$$

$$P_g - P_l = J\frac{df_g}{dt} \tag{5}$$

where H is the kinetic energy of the system normalized to the apparent power of the generator connected to the system.

$$H = \frac{Jf_g^2}{2S_g} \tag{6}$$

Rearranging (5) one can obtain as:

$$\frac{2H}{f_g}\frac{df_g}{dt} = \frac{P_g - P_l}{S_g} \tag{7}$$

In terms of frequency, the equation (7) can be written as:

$$\left(\frac{2H}{f}\right)\frac{df_g}{dt} = \frac{P_g - P_l}{S_g} \tag{8}$$

where df_g/dt is the ROCOF of the system. Before the activation of any controller, the SG releases the inertia stored in the form of kinetic energy due to the rotor mass if an imbalance situation occurs. The duration of this release of inertia is up to 10 s [71]. The primary controller also activates, if the deviation in frequency surpasses a specific value. During the primary response, the power output of the generating units is increased using the governor control to bring the frequency back to normal range within the 30s. If the frequency deviates after the primary control, secondary control is used to regulate the frequency to its nominal value ranging for a few minutes. Finally, the deviation in the remaining power activates the tertiary frequency control.

IV. MHPP MODELING BASED POWER SYSTEM MODELING

This section will explain the modeling of an MHPP with dynamic equations in the synchronous reference frame [2], [73].

A. GRID SIDE MODELING

The three phase grid voltage $e_{g,a\ bc}$ in terms of the impedance $L_{g,e\ q}$ and $R_{g,e\ q}$ between the grid and converter with the current direction toward the converter can be given as follows:

$$e_{g,a\ bc} = R_{g,e\ q}i_{g,a\ bc} + L_{g,e\ q}\frac{di_{g,a\ bc}}{dt} + v_{g,a\ bc} \tag{9}$$

$$C_{dc}\frac{dV_{dc}}{dt} = i_{dc} - i_L \tag{10}$$

The grid voltage $e_{g,a\,bc}$ is represented in synchronous reference frame and given as follows:

$$\begin{bmatrix} e_{gd} \\ e_{gq} \end{bmatrix} = R_{g,e\,q}\begin{bmatrix} i_{gd} \\ i_{gq} \end{bmatrix} + L_{g,e\,q}\frac{d}{dt}\begin{bmatrix} i_{gd} \\ i_{gq} \end{bmatrix} + \omega L_{g,e\,q}\begin{bmatrix} 0 & -1 \\ 1 & 0 \end{bmatrix}\begin{bmatrix} i_{gd} \\ i_{gq} \end{bmatrix} + \begin{bmatrix} v_{gd} \\ v_{gq} \end{bmatrix} \quad (11)$$

The active power and reactive power in terms of the grid voltage and current in synchronous reference frame are given as follows:

$$\begin{bmatrix} P_g \\ Q_g \end{bmatrix} = \frac{3}{2}\begin{bmatrix} v_{gd}i_{gd} \\ -v_{gq}i_{gq} \end{bmatrix} \quad (12)$$

The stored energy in capacitor can be written as follows:

$$E_{dc} = \frac{1}{2}C_{dc}V_{dc}^2 \quad (13)$$

B. MACHINE SIDE MODELING

This section will provide the dynamic modeling of MSC. The dynamic equations of a salient pole rotor filed excited synchronous machine is given as [74]:

$$\begin{bmatrix} e_{sd} \\ e_{sq} \end{bmatrix} = R_s\begin{bmatrix} i_{sd} \\ i_{sq} \end{bmatrix} + \frac{d}{dt}\begin{bmatrix} \lambda_{sd} \\ \lambda_{sq} \end{bmatrix} + \omega\begin{bmatrix} 0 & -1 \\ 1 & 0 \end{bmatrix}\begin{bmatrix} \lambda_{sd} \\ \lambda_{sq} \end{bmatrix} \quad (14)$$

where λ_{sd} and λ_{sq} are dq flux linkages given as follows:

$$\begin{bmatrix} \lambda_{sd} \\ \lambda_{sq} \end{bmatrix} = \begin{bmatrix} L_{sd}i_{sd} \\ L_{sq}i_{sq} \end{bmatrix} + \begin{bmatrix} L_{md}i_{rd} \\ L_{mq}i_{rq} \end{bmatrix} + L_{md}\begin{bmatrix} i_{fd} \\ 0 \end{bmatrix} \quad (15)$$

Here $L_{sd/q}$ is the sum of magnetizing inductance $L_{md/q}$ and leakage inductance L_{ls}. The stator voltages can be further simplified by neglecting the damper winding currents $r_{rd/q}$ given as follows:

$$\begin{bmatrix} e_{sd} \\ e_{sq} \end{bmatrix} = R_s\begin{bmatrix} i_{sd} \\ i_{sq} \end{bmatrix} + \frac{d}{dt}\begin{bmatrix} L_{sd}i_{sd} \\ L_{sq}i_{sq} \end{bmatrix} + \frac{d}{dt}\begin{bmatrix} L_{md}i_{rd} \\ L_{mq}i_{rq} \end{bmatrix} + L_{md}\frac{d}{dt}\begin{bmatrix} i_{fd} \\ 0 \end{bmatrix} + \omega\begin{bmatrix} 0 & -L_{sq} \\ L_{sd} & 0 \end{bmatrix}\begin{bmatrix} i_{sd} \\ i_{sq} \end{bmatrix} + \omega i_{fd}\begin{bmatrix} 0 \\ 1 \end{bmatrix} \quad (16)$$

The converter voltage in terms of the equivalent impedances and the stator voltage equation in (16) in dq-reference frame can be represented as follows:

$$\begin{bmatrix} v_{md} \\ v_{mq} \end{bmatrix} = R_{m,e\,q}\begin{bmatrix} i_{sd} \\ i_{sq} \end{bmatrix} + \frac{d}{dt}\begin{bmatrix} L_{md,e\,q}i_{sd} \\ L_{mq,e\,q}i_{sq} \end{bmatrix} + L_{md}\frac{d}{dt}\begin{bmatrix} i_{fd} \\ 0 \end{bmatrix} + \omega\begin{bmatrix} 0 & -L_{md,e\,q} \\ L_{mq,e\,q} & 0 \end{bmatrix}\begin{bmatrix} i_{sd} \\ i_{sq} \end{bmatrix} + \omega i_{fd}\begin{bmatrix} 0 \\ 1 \end{bmatrix} \quad (17)$$

where the equivalent resistance R_{meq} is the sum of the converter resistance R_{mC} and the stator resistance. The torque and speed relationship of the motor can be expressed by the swing equation given as follows:

$$T_{em-}T_l = J\frac{d\omega_m}{dt} \quad (18)$$

The electromagnetic torque of the motor can be controlled to change the speed of machine. The expression of the electromagnetic torque is expressed as follows:

$$T_{em} = \frac{p}{2}[L_{md}(i_{fd} + i_{rd})i_{sq} + (L_{sd} - L_{sq})i_{sd}i_{sq} - L_{mq}i_{sd}i_{rq}] \quad (19)$$

Neglecting the damper winding current and saliency term $(L_{sd} - L_{sq})i_{sd}i_{sq}$, the expression in (19) can be written as:

$$T_{em} = \frac{p}{2}\left(L_{md}i_{sq}i_{fd}\right) \quad (20)$$

V. INERTIA CONTROL SCHEMES FOR GRID CONNECTED MHPP

This section presents the various techniques presented in the literature to cope with the frequency control problem due to less inertia in the system. The techniques presented in the literature are Classical torque control and VSM.

A. DIRECT TORQUE CONTROL

1) MSC CONTROL

There are several control methodologies to emulated inertia by adding a control loop. The principle of inertia control is to control the speed of the machine by changing the speed or torque such that the kinetic energy is either released or absorbed in proportion to the imbalance in power [75]. After power imbalance, the change in frequency is measured, and then the reference speed is changed according to the change in frequency. The concept of inertia emulation in the MSC can be deduced from (8), which portrays the direct relation between the change in power and change in frequency. The change in power due to load imbalance will affect the frequency of the system. Thus, when the speed of the machine is decreased, it releases the electrical power equivalent to the kinetic inertia of the machine. The control of the deviation in the speed based on ROCOF results in the inertia emulation.

Three main topologies are used to change the reference speed according to the change in frequency. The three methods are: (a) df/dt method, (b) Δf method, and (c) Trigger method as shown in Fig. 9. In df/dt method, the kinetic energy is used to tune the ROCOF multiplied by a gain, as shown in Fig. 9.a. However, this method has the disadvantage of complicated tuning and fluctuations in power [76]. On the other side, the Δf method based on the deviation in frequency has less complication in its implementation, as shown in Fig. 9.b. A most simple topology is the trigger method, as shown in Fig. 9.c. In this method, a trigger is used to release a constant amount of energy if the deviation in frequency reaches a certain level. Thus, inertia can be controlled through any of the above methods or a combination of these methods. The author in [2] combined the df/dt and Δf method to achieve a massive and rapid response to change in frequency, as shown in Fig. 10.

Equation (20) reveals that the torque and speed can be controlled through (i_{sq}), which can be further used to control the voltage. The speed control loop shown in Fig. 10 gener-

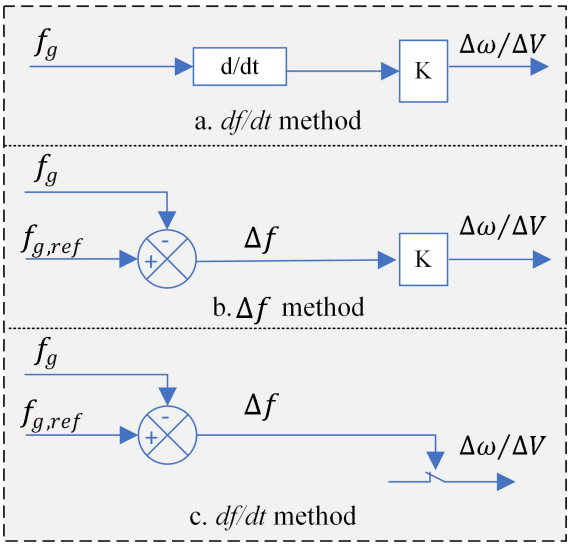

FIGURE 9. Reference speed generation according to frequency variation.

ates reference q-axis current (i^*_{sq}) using three input quantities: (1) reference speed, (b) Actual speed, and (c) inertia controller output. PI control is used to generate the reference voltage from the current error in the d and q axis reference frame due to its simple structure and low cost [77]. The overall operation of the current control is shown in Fig. 10, while the mathematical representation of current control is given as follows:

$$\begin{bmatrix} v^*_{sd} \\ v^*_{sq} \end{bmatrix} = \begin{bmatrix} k_{I,p\ sd} + \dfrac{k_{I,i\ sd}}{s} & 0 \\ 0 & k_{I,p\ sq} + \dfrac{k_{I,i\ sq}}{s} \end{bmatrix} \begin{bmatrix} i^*_{sd} - i_{sd} \\ i^*_{sq} - i_{sq} \end{bmatrix} + \omega \begin{bmatrix} -L_{mq,e\ q} i_{sq} \\ L_{md,e\ q} i_{sd} + i_{fd} L_{md} \end{bmatrix} \quad (21)$$

2) GSC CONTROL

The GSC control adjusts the active power flow to maintain a constant DC link voltage according to the given reference DC voltage. Like the MSC control loop, the GSC control loop consists of outer loop inertia control and DC voltage control loop, and inner loop current control. The inertia emulation is performed in the outer loop by changing the DC link voltage reference. A supplementary inertia control is added with the DC link voltage error to emulate inertia. The concept of the inertia emulation on the grid side can be deduced from the relation between the deviation in the DC voltage and deviation in power. Using (13), the effect of the deviation in a given DC-link voltage on the power can be expressed as follows:

$$\Delta P_{em} = C_{dc} \Delta V_{dc} \quad (22)$$

Thus, a supplementary inertia can be emulated along with the change in DC link voltage using the voltage and power deviation relation expressed in (22).

The outer loop controls the active power using the current error to control the DC link voltage. The control of the DC link voltage is performed in this control loop. To keep the DC link voltage according to the reference value, this control loop will control the active power when there is an increase in power production from the governor's side. The inertia is also emulated in this loop, thus changing the DC link voltage by absorbing or injecting active power. According to (12), it is evident that the active and reactive power is controlled using i_{gd} and i_{gq}, respectively. The relationship between V_{dc} and i_{gd} is given as follows:

$$C_{dc} \frac{d\,(\Delta V_{dc})}{dt} = \frac{3}{2} \frac{\bar{v} \Delta i_{gd}}{V^*_{dc}} \quad (23)$$

Equation (23) reveals that the i_{gd} will change the V_{dc}, thus resulting in the regulation of active power. The decoupled

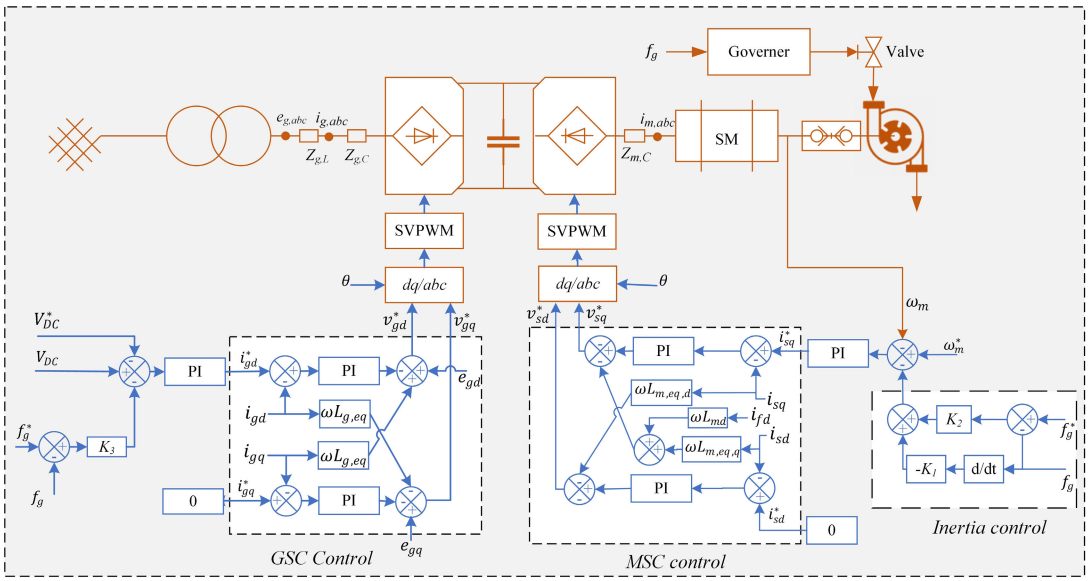

FIGURE 10. Overall DTC scheme using PI control scheme for inertia emulation.

quantities in (11) with PI controller are used to generate reference voltages v_d^* and v_q^* using the current error and the grid voltages given as follows:

$$\begin{bmatrix} v_d^* \\ v_q^* \end{bmatrix} = -\begin{bmatrix} k_{I,p\,d} + \dfrac{k_{I,i\,d}}{s} & 0 \\ 0 & k_{I,p\,q} + \dfrac{k_{I,i\,q}}{S} \end{bmatrix} \begin{bmatrix} i_{gd-}^* i_{gd} \\ i_{gq}^* - i_{gq} \end{bmatrix} + \omega \begin{bmatrix} L_{g,e\,q} i_{gq} \\ -L_{g,e\,q} i_{gd} \end{bmatrix} + \begin{bmatrix} e_{gd} \\ e_{gq} \end{bmatrix} \quad (24)$$

B. VIRTUAL SYNCHRONOUS MACHINE

A VSM is generally used to integrate inverter-based DGs into the grid system using the emulation of an SM in the inverter control part [78]. Nowadays, an SM is one of the dominant types of generators in the electric power grid system due to its premium advantages that are [64], [79]–[81]: (1) to supply kinetic energy stored in the rotor mass as inertia to the grid, (2) it can absorb and supply reactive power, (3) they have a simple and resilient structure with a good grid stabilizing response, (4) flexible operating abilities in both standalone and grid-connected modes, and (5) they can be operated as a single frequency grid when connected in parallel. Many researchers used such abilities of SM in the control of converters to integrated inverter-based DGs. The control system proposed in the literature under names such as VSM [82], VISMA [83], synchro converter [84], [85], eVSM [86], and so on [87]–[89]. Beck and Hesse were the first to propose the idea of VSM, labeling it as VISMA [83], in which they proposed a model of the damper windings at the actual circuit level. But the proposed technique has some limitations due to higher model complexity and the unknown ability of the proposed VSM to damp oscillations beyond a normal SM. Subsequently, several VSM has been proposed, adopting various ways to model the effect of damping with a wide range of complexities. The VSM control topology can be divided into two models: (a) High order models (HOMs) [90]–[92] and (b) Low order models (LOMs) [93]–[96]. The HOMs represent the full model of SM and are relatively complex as compared to LOMs. Most of the researcher only considers the mechanical part of the SM to proposed VSMs. The electrical part has also been included throughout the relation between stator current and voltage, as reported in [97]. This results in a full order model of an SM with 5th order electrical part and 2nd order mechanical part [98].

Furthermore, the author in [99] classified the VSM based on damping, the one that applies damping effect in (1) speed or real power loop, and (2) reactive power or magnitude loop. On the other hand, the synchro converter works on the difference between the nominal speed and virtual speed in the real power loop. The swing equation of the SM has characteristics of inertia and damping. The dominant behavior of SM can be modeled to calculate the phase angle from the power error. Considering the swing equation of SM, several control paradigms have been presented in the literature to allow integrate the virtual or synthetic inertia to the grid using power converters for a wide range of applications [85], [98], [100]–[105].

In this section, the frequency control of the MHPP is presented using VSM. The classical torque control is modified to integrate the control characteristics of VSM, as presented in [2]. The VSM is presented with PLL [106] and without PLL [2]. The overall control consists of the GSC control loop and MSC control loop. The speed control is performed using the governor; the DC link voltage control is done in the MSC control loop, whereas the active power is controlled in the GSC control loop. The overall operation of the VSM is shown in Fig. 11.

1) GSC CONTROL WITH PLL

The main difference between the conventional control scheme and VSM based control system for power converters is the rotating inertia emulation and the virtual inertia synchronization methodology based on power balancing. The swing equation linearized with respect to speed is used to implement VSM. This swing equation represents the damping and inertia of a traditional SM and the power balance is used to determine the acceleration of inertia [98], [107] given as:

$$T_a \frac{d}{dt} f_{vsm} = P^{r*} - P - P_d \quad (25)$$

where $P_d = k_d\,(f_{vsm} - f_{PLL})$, and the f_{PLL} is estimated value of actual grid frequency calculated using a phase-locked loop (PLL). The power frequency droop effect is incorporated using a droop constant k_w acting on the change in VSM speed given as $\left(f_{vsm} - f_{vsm}^*\right)$. Hence the virtual mechanical input power P^{r*} in terms of frequency droop effect and external reference power can be expressed as:

$$P^{r*} = P_g{}^* + k_w \left(f_{vsm} - f_{vsm}^*\right) \quad (26)$$

The phase angle of the VSM in steady-state condition should be constant during grid-connected mode to model the VSM in SRF and should correspond to the phase displacement between grid voltage vector and VSM internal voltage vector virtual position. For this purpose, the deviation of VSM speed from grid actual frequency is modeled by introducing a new variable in the form of speed deviation Δf_{vsm} and the corresponding change in phase angle $\delta\theta_{vsm}$. Thus, the resulting power balance equation and the corresponding change in angle by introducing Δf_{vsm} and $\delta\theta_{vsm}$ can be expressed as:

$$T_a \frac{d}{dt} \Delta f_{vsm} = \left(P^* - k_w \left(f_{vsm} - f_{vsm}^*\right)\right) - P - k_d\,(f_{vsm} - f_{PLL}) \quad (27)$$

$$\frac{d}{dt} \delta\theta_{vsm} = \Delta f_{vsm} \cdot \omega_b \quad (28)$$

The original grid frequency and the corresponding phase angle that will be used as a transformation angle between the rotating reference frame defined by three-phase quantities and VSM inertia are given as:

$$f_{vsm} = \Delta f_{vsm} + f_g$$
$$\frac{d}{dt} \theta_{vsm} = f_{vsm} \cdot \omega_b$$

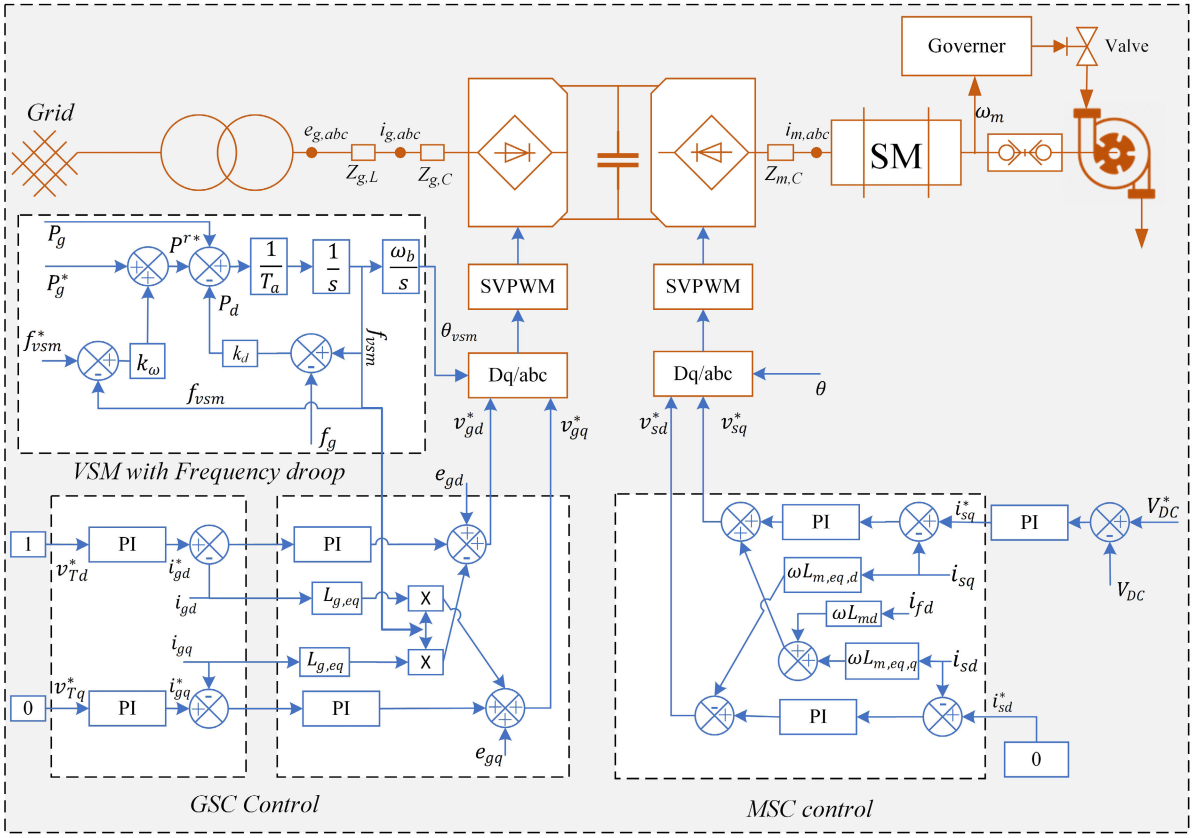

FIGURE 11. VSM scheme for inertia emulation.

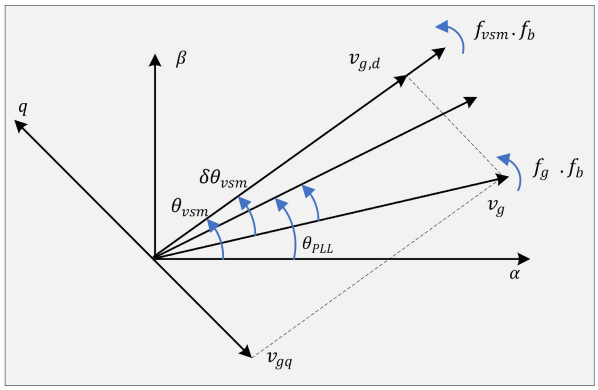

FIGURE 12. Synchronous reference frame for PLL based VSM.

Once the VSM is in a steady-state condition, the grid frequency becomes equal to the VSM frequency, and hence $\delta\theta_{vsm} = 0$.

The phase angle θ_{vsm}, that is used in the reference frame transformation between VSM oriented synchronous reference frame (VSM-SRF) and stationary reference frame, is responsible for the synchronization of grid and VSM control scheme. During steady state condition, the frequency of the VSM-SRF is same as the grid voltage, thus the phase angle will variate between 0 and 2π, whereas the phase difference between the two aforementioned quantities is denoted by $\delta\theta_{vsm}$. Thus using this VSM-SRF, the electrical system modeling and control is performed, thus avoiding the need for multiple transformation between the local reference frame for control and global reference frame for electrical system modeling [106]. Thus, the grid voltage is this VSMSRF can be shown as:

$$v_g = \hat{v}_g e^{-j\delta\theta_{vsm}} \tag{29}$$

As the VSM damping effect is implemented using estimated grid frequency, thus the filter capacitor voltage v_0 is introduced to implement the PLL and PLL will then operate on its own established SRF aligned with the voltage vector v_0. The resulting phase difference is labelled as $\delta\theta_{PLL}$ and the overall reference frame is shown in Fig. 12 [106]. The voltage vector v_0 in the PLL oriented frame can be expressed as:

$$v_0^{PLL} = v_0^{VSM} e^{-j(\delta\theta_{PLL} - \delta\theta_{vsm})} \tag{30}$$

The structure of PLL to track the actual grid frequency is shown in Fig. 13 and its structure based on [108], [109]. A PI controller taking the phase angle error as input is used to track the voltage frequency, which is then integrated to obtain the actual phase angle θ_{PLL}. The filtered voltage v_{PLL} with $f_{LP,P\,LL}$ as cut-off frequency for low-pass filter is given as:

$$\frac{d}{dt} v_{PLL} = -f_{LP,P\,LL} \cdot v_{PLL} + f_{LP,P\,LL} \cdot v_0 e^{-j(\delta\theta_{PLL} - \delta\theta_{vsm})} \tag{31}$$

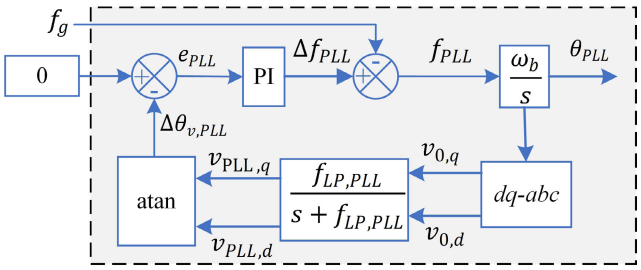

FIGURE 13. PLL scheme for grid frequency estimation.

The integrator state ε_{PLL} of the PI controller can then be defined by:

$$\frac{d}{dt}\varepsilon_{PLL} = \tan^{-1}\left(\frac{v_{q,P\,LL}}{v_{d,P\,LL}}\right) \tag{32}$$

The change in the speed and phase angle of grid frequency with respect to VSM speed is expressed as:

$$\Delta f_{PLL} = k_{p,P\,LL}\cdot\tan^{-1}\left(\frac{v_{q,P\,LL}}{v_{d,P\,LL}}\right) + k_{i,P\,LL}\cdot\varepsilon_{PLL} \tag{33}$$

$$\frac{d}{dt}\delta\theta_{PLL} = \Delta f_{PLL}\cdot\omega_b \tag{34}$$

The actual per unit frequency f_{PLL}, estimated using the PLL and the corresponding phase angle is given as follows:

$$f_{PLL} = \Delta f_{PLL} + f_g \tag{35}$$

$$\frac{d}{dt}\theta_{PLL} = f_{PLL}\cdot\omega_b \tag{36}$$

A PI control also used here to generate the reference current from the converter terminal voltages v_T in d and q axis reference frame due to its simple structure and low cost [77]. The overall operation of the current control is shown in Fig.11 while the mathematical representation of current control is given as follows:

$$\begin{bmatrix} i^*_{sd} \\ i^*_{sq} \end{bmatrix} = -\begin{bmatrix} k_{v,p\,d} + \frac{k_{v,i\,d}}{s} & 0 \\ 0 & k_{v,p\,q} + \frac{k_{v,i\,q}}{s} \end{bmatrix}\begin{bmatrix} v_{Td} - v_{Td}{}^* \\ v^*_{Tq} - v_{Tq} \end{bmatrix} \tag{37}$$

The error between the above reference current and actual current is used to generate reference voltages using PI control scheme. The overall topology including the current control and voltage control is shown in Fig. 11.

$$\begin{bmatrix} v^*_{gd} \\ v^*_{gq} \end{bmatrix} = -\begin{bmatrix} k_{I,p\,d} + \frac{k_{I,i\,d}}{s} & 0 \\ 0 & k_{I,p\,q} + \frac{k_{I,i\,q}}{s} \end{bmatrix}\begin{bmatrix} i^*_{gd} - i_{gd} \\ i^*_{gq} - i_{gq} \end{bmatrix} + f_{vsm}\begin{bmatrix} L_{g,e\,q} i_{gq} \\ -L_{g,e\,q} i_{gd} \end{bmatrix} + \begin{bmatrix} e_{gd} \\ e_{gq} \end{bmatrix} \tag{38}$$

2) MSC CONTROL

The MSC control in VSM case is different than that in the case of classical torque control as shown in Fig. 10. It consists of an outer voltage loop and inner current loop. The inner current loop is implemented like classical torque control loop, whereas the outer voltage loop takes the difference between DC link voltage and reference DC link voltage to control the active power using reference i^*_{sq} given as follows:

$$\begin{bmatrix} i^*_{sd} \\ i^*_{sq} \end{bmatrix} = -\begin{bmatrix} 0 & 0 \\ k_{V,p} + \frac{k_{V,i}}{s} & 0 \end{bmatrix}\begin{bmatrix} v^*_{DC} - v_{DC} \\ 0 \end{bmatrix} \tag{39}$$

C. VSM WITH POWER-FREQUENCY PD CONTROLLER

A power controller can be added to the VSM to bring the power back to its reference value. Thus a proportional differential (PD) concept is used to generated reference power P^*_g. The addition of PD control to the P^*_r in (26) will adjust the reference power to the VSM and the MHPP will contribute to the reference power even under grid frequency deviations. The new term P_{r-PD} is given as follows:

$$P_{r-PD} = k_p\,(f_{vsm} - f_{PLL}) + \frac{k_d\,(f_{vsm})\,s}{s + f_{vsm}}\,(f_{vsm} - f_{PLL}) \tag{40}$$

D. VSM WITH POWER-FREQUENCY PID CONTROLLER AND PERMANENT DROOP

To further make the system robust, the VSM can be combined with the proportional integral differential (PID) concept. The PID will act as conventional MHPP governor and the frequency response will be much robust as compared to proportional based VSM. The updated P_d is given as follow:

$$P_{rpID} = k_p\epsilon + \frac{k_d\,(f_{vsm})\,s}{s + f_{vsm}}\epsilon + \frac{k_i}{s}\epsilon$$
$$\epsilon = (f_{vsm} - f_{PLL} - Pf) \tag{41}$$

E. NONLINEAR MODEL PREDICTIVE CONTROL

The synthetic inertia emulation and control schemes discussed in previous sections are based on P, PI, PD, and PID. Certain constraints in the MHPP system need to be fulfilled for the smooth operation of the overall control paradigm. The constraints include certain operating limits of hydraulic and electric variables. Besides this, the turbine control should be robust to stabilize the grid through fast frequency reserves (FFR) obtained using the kinetic energy of SG within the constraints. A conventional PID controller damages the power system because it becomes slow due to careful tuning for fulfilling these constraints. Therefore, a more advanced system based on MPC is designed in [110] to meet the constraint and maximize the efficiency of the power system. The authors utilized an 11 bus Kundur two area system [73] integrated with an MHPP. The difference between previous techniques and MPC based scheme is that the reference power P^*_g and the guide vane opening reference g^* is calculated using the MPC scheme, as shown in Fig. 14. The MPC is then combined with the VSM to provide optimized frequency and power oscillation damping support.

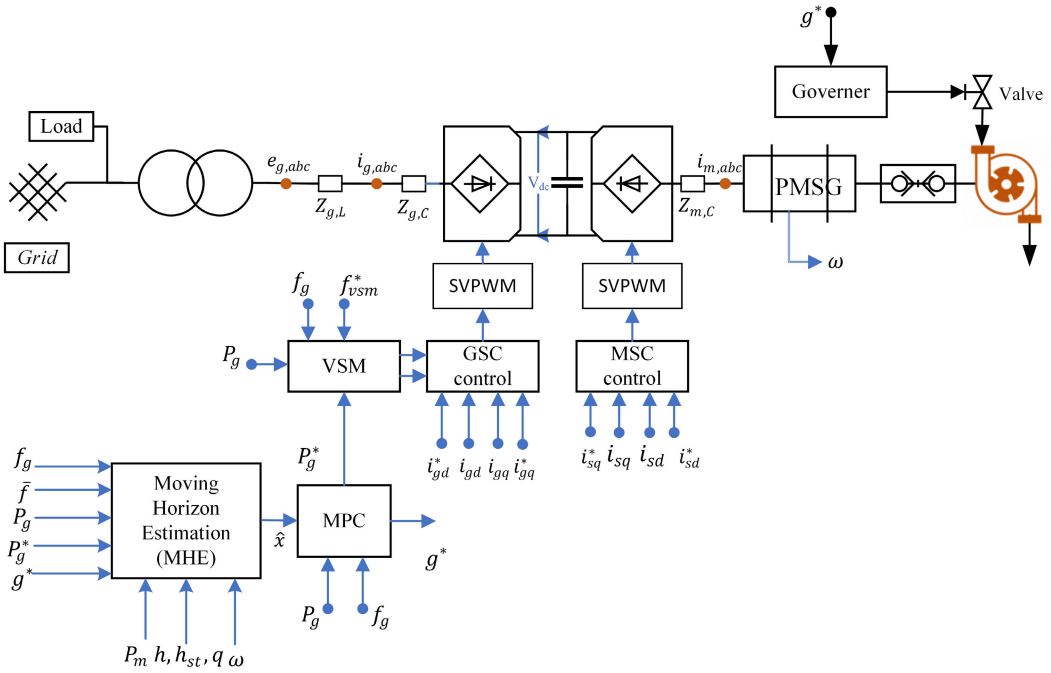

FIGURE 14. MPC based inertia emulation control for MHPP.

TABLE 2. Performance analysis in terms of various dynamics.

Control techniques	Complexity	Robustness	Advantages	Limitations
DTC	Low Complexity	Slower	- provides better decoupling of flux and torque - Computationally efficient - no coordinate transformation requirements - better dynamic response	- current and torque ripples are high - current THD is high - poor power quality - switches failure problems due to variable switching frequency
VSM with PLL	Medium	Fast	- can be implemented based on 5^{th}, 7^{th}, order and phasor model of SM - can be implemented in rectification mode to make a unified interface for smart grid - control parameters are flexible -can be implemented as current and voltage controlled source	-can be influenced by nonlinear high frequency harmonics -no specific principles to select the VSM parameters - doesn't incorporates external effects
VSM combined with power frequency PD and PID controller	Medium	Fast	-provides improved frequency response -adds the power control to the inertia control -imitates the function of governor	-number of tuning parameters is increased -high complexity -doesn't incorporates external effects
MPC	High Complexity	Slower	-implementation is easy - no tuning parameters - cost function is flexible - constraints can be select according to operating environment -replaces governor control by the guide vane effect of water hammering can be included damping effect of power oscillation is included	- problem formulation is difficult - complex constraints selection - slack variables addition - controller time delay - realistic selection of hydraulic system

MPC uses the dynamic model of the system to formulate an optimization problem and then uses the current state of the plant to generate optimal control sequence and then apply this sequence to the system as input [111]. The significant contribution of the MPC based MHPP control presented in [110] are: (1) Primary frequency control, (2) Hydraulic system control, and (3) Turbine speed control. In primary frequency control, reference power P^*_g is generated and then provided as input to VSM to minimize the variation in the grid frequency, oscillation damping, and keeping the converter power within certain limits. In hydraulic system control, an optimal guide vane reference g^* is generated and then provide as an input to the governor. This optimal value of g^* will provide optimal control and reduce the guide vane operation to minimize wear and tear, water hammering, and mass oscillations. The surge tank head h_{st} is kept within the operating limits, and also the water flow q is kept above its minimum level. The turbine speed is also kept at the optimal

value and is controlled to recover itself after any disturbance. To achieve the aforementioned objectives, a quadratic objective function with non-linearly equal and linearly equal constraint are used [110] given as follows:

$$\begin{aligned}&\min_{x\in\mathbb{R}^n,\ u\in\mathbb{R}^m} f(x,u)\\&=\sum_{t=0}^{N-1}\frac{1}{2}x_{t+1}^{\mathrm{T}}Q_{t+1}x_{t+1}\\&\quad+d_{xt+1}x_{t+1}+\frac{1}{2}\Delta x_{t+1}^{\mathrm{T}}Q_{\Delta t}\Delta x_{t+1}+\frac{1}{2}u_t^{\mathrm{T}}R_t u_t\\&\quad+d_{ut}u_t+\frac{1}{2}\Delta u_t^{\mathrm{T}}R_{\Delta t}\Delta u_t+\rho^{\mathrm{T}}\epsilon_t+\frac{1}{2}\epsilon_t^{\mathrm{T}}S\epsilon_t\end{aligned}\quad(42)$$

where x $= [\Delta f, g, q, q_{hr}, h_{st}, \omega_m]$. The constraints defined for the optimization problems are the guide vane opening reference g^* that ranges between 0.1 and 1.2 and the converter power P_G between 0 and 1. Moreover, a number of slack variables have been added to the MPC problem that includes the water flow q, surge tank head h_{st}, turbine head h, and rotating speed of turbine ω. A multi-variable algorithm known as moving horizon estimation (MHE) is also utilized to estimate the current states (x) using the dynamic model of the plant.

The techniques reviewed in this article has certain advantages and disadvantages. A comprehensive comparison of the reviewed techniques is presented in table 2 portraying the complexity, advantages, disadvantages and robustness against the load variation.

VI. CONCLUSION AND FUTURE WORK

This paper presents the various control paradigm developments in recent years for micro-hydro power plants (MHPP) efficient control in grid-connected and standalone modes. A detailed literature review of the control techniques for MHPP in standalone mode is presented. The frequency control for standalone MHPP during power imbalance using fuzzy logic control and PI control is reviewed. The concepts for inertia emulation and its utilization in the frequency control during the load imbalance in grid-connected mode are presented. The latest techniques for the grid-connected mode mathematically presented in this paper include direct torque control, virtual synchronous machine (VSM), model predictive control, and VSM with PD and PID control. The advantages and disadvantages of all the reviewed techniques are also presented. These techniques are quite mature for wind energy and solar photovoltaic systems, but no valuable research has been done for MHPPs. The direct torque control (DTC) can be further enhanced by incorporating robust techniques like sliding mode control and its variants. Further research is also needed for the internal parameters of the VSM. Multiple VSMs can also be implemented to improve the performance of MHPPs in the presence of damping, inertia, power, and voltage loops. Some robust techniques like adaptive fuzzy [112] control and battery energy storage system with consensus [113] can be incorporated with synthetic inertia emulation techniques. The effect of power converters and its overloading capability in the context of VSM based MHPP can also be explored for further research work. In the near future, the implementation of these techniques will be done to provide detailed comparison and challenges in implementing reviewed techniques.

REFERENCES

[1] H. Bevrani, T. Ise, and Y. Miura, "Virtual synchronous generators: A survey and new perspectives," *Int. J. Electr. Power Energy Syst.*, vol. 54, pp. 244–254, Jan. 2014.
[2] M. Gallefoss, "Synthetic inertia from a converter-fed synchronous machine in a hydro-electric power plant-modeling, control and analysis," M.S. thesis, NTNU, Trondheim, Norway, 2018. [Online]. Available: http://hdl.handle.net/11250/2561565
[3] M. Dreidy, H. Mokhlis, and S. Mekhilef, "Inertia response and frequency control techniques for renewable energy sources: A review," *Renew. Sustain. Energy Rev.*, vol. 69, pp. 144–155, Mar. 2017.
[4] A. V. Jayawardena, L. G. Meegahapola, S. Perera, and D. A. Robinson, "Dynamic characteristics of a hybrid microgrid with inverter and non-inverter interfaced renewable energy sources: A case study," in *Proc. IEEE Int. Conf. Power Syst. Technol. (POWERCON)*, Oct. 2012, pp. 1–6.
[5] K. Koyanagi, Y. Hida, Y. Ito, K. Yoshimi, R. Yokoyama, M. Inokuchi, T. Mouri, and J. Eguchi, "A smart photovoltaic generation system integrated with lithium-ion capacitor storage," in *Proc. 46th Int. Univ. Power Eng. Conf. (UPEC)*, 2011, pp. 1–6.
[6] H. Bevrani and T. Hiyama, *Intelligent Automatic Generation Control*. Boca Raton, FL, USA: CRC Press, 2017.
[7] B. P. Roberts and C. Sandberg, "The role of energy storage in development of smart grids," *Proc. IEEE*, vol. 99, no. 6, pp. 1139–1144, Jun. 2011.
[8] J. A. Suul, "Variable speed pumped storage hydropower plants for integration of wind power in isolated power systems," in *Renewable Energy*. London, U.K.: IntechOpen, 2009.
[9] U. Tamrakar, D. Shrestha, M. Maharjan, B. Bhattarai, T. Hansen, and R. Tonkoski, "Virtual inertia: Current trends and future directions," *Appl. Sci.*, vol. 7, no. 7, p. 654, Jun. 2017.
[10] R. R. Singh, B. A. Kumar, D. Shruthi, R. Panda, and C. T. Raj, "Review and experimental illustrations of electronic load controller used in standalone micro-hydro generating plants," *Eng. Sci. Technol., Int. J.*, vol. 21, no. 5, pp. 886–900, Oct. 2018.
[11] S. Doolla, T. S. Bhatti, and R. C. Bansal, "Load frequency control of an isolated small hydro power plant using multi-pipe scheme," *Electr. Power Compon. Syst.*, vol. 39, no. 1, pp. 46–63, Jan. 2011.
[12] J. L. Woodward and J. T. Boys, "Electronic load governor for small hydro plants," in *Proc. Water Power Dam Construct.*, Jul. 1980, pp. 37–39.
[13] S. Kormilo and P. Robinson, "Electronic control of small hydroelectric schemes using a microcomputer," *IEE Proc. E—Comput. Digit. Techn.*, vol. 131, no. 4, pp. 132–136, Jul. 1984.
[14] R. Bonert and G. Hoops, "Stand alone induction generator with terminal impedance controller and no turbine controls," *IEEE Trans. Energy Convers.*, vol. 5, no. 1, pp. 28–31, Mar. 1990.
[15] P. Freere, "Electronic load/excitation controller for a self-excited squirrel cage generator micro-hydro scheme," in *Proc. 5th Int. Conf. Elect. Mach. Drives*, 1991, pp. 266–270.
[16] M. Chennani, I. Salhi, and S. Doubabi, "Study of the regulation of a micro hydroelectric power plant prototype," *Int. Sci. J. Alternative Energy Ecol.*, vol. 5, no. 6, pp. 79–84, 2008.
[17] S. Pokhrel, P. Parajuli, and B. Adhikary, "Design and performance of lab fabricated induction generator controller," in *Proc. 2nd Int. Conf. Develop. Renew. Energy Technol. (ICDRET)*, 2012, pp. 1–3.
[18] J. Portegijs. (2000). *The Humming Bird' Electronic Load Controller/Induction Generator Controller*. Accessed: Sep. 25, 2020. [Online]. Available: http://microhydropower.net/mhp_group/portegijs/humbird/humb_main.html
[19] W. Jun and Y. Bo, "A novel electronic load controller: Theory and implementation," in *Proc. 5th Int. Conf. Electr. Mach. Syst. (ICEMS)*, vol. 2, 2001, pp. 1276–1278.
[20] I. Salhi, S. Doubabi, N. Essounbouli, and A. J. Hamzaoui, "Application of multi-model control with fuzzy switching to a micro hydro-electrical power plant," *Renew. Energy*, vol. 35, no. 9, pp. 2071–2079, 2010.

[21] S. Gao, S. S. Murthy, G. Bhuvaneswari, and M. S. L. Gayathri, "Design of a microcontroller based electronic load controller for a self excited induction generator supplying single-phase loads," *J. Power Electron.*, vol. 10, no. 4, pp. 444–449, Jul. 2010.

[22] A. Safaei, H. M. Roodsari, and H. A. Abyaneh, "Optimal load frequency control of an island small hydropower plant," in *Proc. 3rd Conf. Thermal Power Plants*, 2011, pp. 1–6.

[23] I. Salhi, S. Doubabi, N. Essounbouli, and A. Hamzaoui, "Frequency regulation for large load variations on micro-hydro power plants with real-time implementation," *Int. J. Electr. Power Energy Syst.*, vol. 60, pp. 6–13, Sep. 2014.

[24] S. S. Murthy, Ramrathnam, M. S. L. Gayathri, K. Naidu, and U. Siva, "A novel digital control technique of electronic load controller for SEIG based micro hydel power generation," in *Proc. Int. Conf. Power Electron., Drives Energy Syst.*, Dec. 2006, pp. 1–5.

[25] E. G. Marra and J. A. Pomilio, "Self-excited induction generator controlled by a VS-PWM bidirectional converter for rural applications," *IEEE Trans. Ind. Appl.*, vol. 35, no. 4, pp. 877–883, 1999.

[26] U. K. Kalla, B. Singh, and S. S. Murthy, "Modified electronic load controller for constant frequency operation with voltage regulation of small hydro-driven single-phase SEIG," *IEEE Trans. Ind. Appl.*, vol. 52, no. 4, pp. 2789–2800, Jul. 2016.

[27] G. K. Kasal and B. Singh, "Zig-zag transformer based voltage controller for an isolated asynchronous generator," in *Proc. IEEE Region Conf. (TENCON)*, Nov. 2008, pp. 1–6.

[28] G. Kumar Kasal and B. Singh, "VSC with zig-zag transformer based decoupled controller for a pico hydro power generation," in *Proc. Annu. IEEE India Conf.*, vol. 2, Dec. 2008, pp. 441–446.

[29] B. Singh, G. K. Kasal, A. Chandra, and K. Al-Haddad, "Voltage and frequency controller for an autonomous micro hydro generating system," in *Proc. IEEE Power Energy Soc. Gen. Meeting-Convers. Del. Electr. Energy 21st Century*, Jul. 2008, pp. 1–9.

[30] B. Singh, G. K. Kasal, A. Chandra, and Kamal-Al-Haddad, "A frequency based electronic load controller for an isolated asynchronous generator feeding 3-phase 4-wire loads," in *Proc. IEEE Int. Symp. Ind. Electron.*, Jun. 2008, pp. 1513–1518.

[31] G. K. Kasal and B. Singh, "Decoupled voltage and frequency controller for isolated asynchronous generators feeding three-phase four-wire loads," *IEEE Trans. Power Del.*, vol. 23, no. 2, pp. 966–973, Apr. 2008.

[32] B. Singh, G. K. Kasal, A. Chandra, and Kamal-Al-Haddad, "An independent active and reactive power control of an isolated asynchronous generator in 3-phase 4-wire applications," in *Proc. IEEE Power Electron. Spec. Conf.*, Jun. 2008, pp. 2057–2063.

[33] R. R. Chilipi, S. S. Murthy, S. Madishetti, B. Singh, and G. Bhuvaneswari, "Design and implementation of dynamic electronic load controller for three-phase self-excited induction generator in remote small-hydro power generation," *IET Renew. Power Gener.*, vol. 8, no. 3, pp. 269–280, Apr. 2014.

[34] S. Gao, G. Bhuvaneswari, S. S. Murthy, and U. Kalla, "Efficient voltage regulation scheme for three-phase self-excited induction generator feeding single-phase load in remote locations," *IET Renew. Power Gener.*, vol. 8, no. 2, pp. 100–108, Mar. 2014.

[35] R. Bonert and S. Rajakaruna, "Self-excited induction generator with excellent voltage and frequency control," *IEE Proc.—Gener., Transmiss. Distrib.*, vol. 145, no. 1, pp. 33–39, Jan. 1998.

[36] J. M. Ramirez and M. E. Torres, "An electronic load controller for self-excited induction generators," in *Proc. IEEE Power Eng. Soc. Gen. Meeting*, Jun. 2007, pp. 1–8.

[37] E. Torres, F. Chan, J. Ramirez, and A. Cowo, "A PWM control for electronic load controller for self-excited induction generator based in IGBT series-inverted switch," in *Proc. 12th IEEE Int. Power Electron. Congr.*, Aug. 2010, pp. 61–66.

[38] B. Singh, S. S. Murthy, and S. Gupta, "An improved electronic load controller for self-excited induction generator in micro-hydel applications," in *Proc. 29th Annu. Conf. IEEE Ind. Electron. Soc. (IECON)*, vol. 3, Nov. 2003, pp. 2741–2746.

[39] R. R. Chilipi, B. Singh, and S. S. Murthy, "Performance of a self-excited induction generator with DSTATCOM-DTC drive-based voltage and frequency controller," *IEEE Trans. Energy Convers.*, vol. 29, no. 3, pp. 545–557, Sep. 2014.

[40] B. Singh, S. S. Murthy, and S. Gupta, "Analysis and implementation of an electronic load controller for a self-excited induction generator," *IEE Proc.—Gener., Transmiss. Distrib.*, vol. 151, no. 1, pp. 51–60, Jan. 2004.

[41] B. Singh and G. Kumar Kasal, "Decoupled voltage and frequency controller for an isolated pico hydro system feeding dynamic loads," in *Proc. 7th Int. Conf. Power Electron.*, Oct. 2007, pp. 1139–1144.

[42] T. Ahmed, K. Nishida, and M. Nakaoka, "A novel stand-alone induction generator system for AC and DC power applications," in *Proc. 14th IAS Annu. Meeting Conf. Rec. Ind. Appl. Conf.*, vol. 4, 2005, pp. 2950–2957.

[43] B. Singh and V. Rajagopal, "Power balance theory based control of an electronic load controller for an isolated asynchronous generator driven by uncontrolled pico hydro turbine," in *Proc. Annu. IEEE India Conf.*, Dec. 2009, pp. 1–5.

[44] F. D. Wijaya, T. Isobe, J. A. Wiik, and R. Shimada, "Terminal voltage control of stand alone induction generator using controlled shunt capacitor called SVC MERS," in *Proc. 13th Eur. Conf. Power Electron. Appl.*, 2009, pp. 1–10.

[45] F. Wijaya, T. Isobe, and R. Shimada, "Study on voltage controller of self-excited induction generator using controlled shunt capacitor, SVC magnetic energy recovery switch," *Jurnal Otomasi, Kontrol, dan Instrumentasi*, vol. 1, no. 2, p. 107, 2011.

[46] D. Guha, P. K. Roy, and S. Banerjee, "Load frequency control of large scale power system using quasi-oppositional grey wolf optimization algorithm," *Eng. Sci. Technol., Int. J.*, vol. 19, no. 4, pp. 1693–1713, 2016.

[47] D. Guha, P. K. Roy, and S. Banerjee, "Quasi-oppositional differential search algorithm applied to load frequency control," *Eng. Sci. Technol., Int. J.*, vol. 19, no. 4, pp. 1635–1654, Dec. 2016.

[48] M. Sruthi, C. Nagamani, and G. S. Ilango, "An improved algorithm for direct computation of optimal voltage and frequency for induction motors," *Eng. Sci. Technol., Int. J.*, vol. 20, no. 5, pp. 1439–1449, 2017.

[49] A. Yadav and A. Appan, "Steady-state analysis of electronic load controller for three phase alternator," in *Proc. Annu. IEEE India Conf. (INDICON)*, Dec. 2015, pp. 1–6.

[50] R. Dahal, S. K. Jha, and B. Adhikary, "Performance of droop based load controller in interconnected micro hydro power plants," in *Proc. 4th Int. Conf. Develop. Renew. Energy Technol. (ICDRET)*, 2016, pp. 1–5.

[51] P. J. Reddy and S. Singh, "Voltage and frequency control of parallel operated synchronous and induction generators in micro hydro scheme," in *Proc. Int. Conf. Comput. Power, Energy, Inf. Commun. (ICCPEIC)*, 2014, pp. 124–129.

[52] K. T. K. Teo, H. H. Goh, B. L. Chua, S. K. Tang, and M. K. Tan, "Modelling and optimisation of stand alone power generation at rural area," in *Proc. IEEE Int. Conf. Consum. Electron.-China*, Apr. 2013, pp. 51–56.

[53] N. Gyawali, B. Paudel, and B. Subedi, "Improved active power sharing strategy for ELC controlled synchronous generators based islanded micro grid application," in *Proc. 9th Int. Conf. Softw., Knowl., Inf. Manage. Appl. (SKIMA)*, 2015, pp. 1–5.

[54] A. Ali, M. U. R. Siddiqi, R. Muhammad, M. Suleman, and N. J. Ullah, "Design and implementation of an electromechanical control system for micro-hydropower plants," *Electr. Eng.*, vol. 102, pp. 891–898, Jan. 2020.

[55] R. Raja Singh, T. Raj Chelliah, and P. Agarwal, "Power electronics in hydro electric energy systems—A review," *Renew. Sustain. Energy Rev.*, vol. 32, pp. 944–959, Apr. 2014.

[56] W. Koczara, Z. Chlodnicki, E. Ernest, A. Krasnodebski, R. Seliga, N. L. Brown, B. Kaminski, and J. Al-Tayie, "Theory of the adjustable speed generation systems," *COMPEL–Int. J. Comput. Math. Elect. Electron. Eng.*, vol. 27, no. 5, pp. 1162–1177, 2008, doi: 10.1108/03321640810890834.

[57] R. M. Dell and D. A. J. Rand, "Energy storage—A key technology for global energy sustainability," *J. Power Sources*, vol. 100, nos. 1–2, pp. 2–17, 2001.

[58] A. Evans, V. Strezov, and T. J. Evans, "Assessment of utility energy storage options for increased renewable energy penetration," *Renew. Sustain. Energy Rev.*, vol. 16, no. 6, pp. 4141–4147, 2012.

[59] A. Joseph, T. R. Chelliah, S. S. Lee, and K.-B. Lee, "Reliability of variable speed pumped-storage plant," *Electronics*, vol. 7, no. 10 p. 265, 2018.

[60] P. K. Steimer, O. Senturk, S. Aubert, and S. Linder, "Converter-fed synchronous machine for pumped hydro storage plants," in *Proc. IEEE Energy Convers. Congr. Expo. (ECCE)*, Sep. 2014, pp. 4561–4567.

[61] M. Valavi and A. Nysveen, "Variable-speed operation of hydropower plants: Past, present, and future," in *Proc. 27th Int. Conf. Electr. Mach. (ICEM)*, Sep. 2016, pp. 640–646.

[62] L. Koedding, "Modern design for variable speed motor generators," in *Proc. SHF Conf.*, 2014.

[63] B. Guo, S. Bacha, M. Alamir, and A. Mohamed, "Variable speed micro-hydro power generation system: Review and Experimental results," in *Proc. Symp. Génie Electr. (SGE)*, 3rd ed. Nancy, France, Jul. 2018.
[64] P. Kundur, N. J. Balu, and M. G. Lauby, *Power System Stability and Control*. New York, NY, USA: McGraw-Hill, 1994.
[65] R. Marquardt, A. Lesnicar, and J. Hildinger, "Modulares stromrichterkonzept für netzkupplungsanwendung bei hohen spannungen," in *Proc. ETG-Fachtagung*, Bad Nauheim, Germany, vol. 114, 2002, pp. 155–161.
[66] M. Hagiwara, K. Nishimura, and H. Akagi, "A medium-voltage motor drive with a modular multilevel PWM inverter," *IEEE Trans. Power Electron.*, vol. 25, no. 7, pp. 1786–1799, Jul. 2010.
[67] N. Mohan, *First Course on Power Systems*. Mesa, AZ, USA: Mnpere, 2006.
[68] Y. Chen, R. Hesse, D. Turschner, and H.-P. Beck, "Investigation of the virtual synchronous machine in the island mode," in *Proc. 3rd IEEE PES Innov. Smart Grid Technol. Eur. (ISGT Europe)*, Oct. 2012, pp. 1–6.
[69] J. Modarresi, E. Gholipour, and A. Khodabakhshian, "A comprehensive review of the voltage stability indices," *Renew. Sustain. Energy Rev.*, vol. 63, pp. 1–12, Sep. 2016.
[70] E. Ørum, M. Kuivaniemi, M. Laasonen, A. I. Bruseth, E. A. Jansson, A. Danell, K. Elkington, and N. Modig, "Future system inertia," ENTSOE, Brussels, Belgium, Tech. Rep., 2015. Accessed: Sep. 25, 2020. [Online]. Available: https://eepublicdownloads.azureedge.net/cleandocuments/Publications/SOC/Nordic/Nordic_report_Future_System_Inertia.pdf
[71] F. M. Gonzalez-Longatt, "Effects of the synthetic inertia from wind power on the total system inertia: Simulation study," in *Proc. 2nd Int. Symp. Environ. Friendly Energies Appl.*, Jun. 2012, pp. 389–395.
[72] F. Díaz-González, M. Hau, A. Sumper, and O. Gomis-Bellmunt, "Participation of wind power plants in system frequency control: Review of grid code requirements and control methods," *Renew. Sustain. Energy Rev.*, vol. 34, pp. 551–564, Jun. 2014.
[73] T. I. Reigstad and K. Uhlen, "Variable speed hydropower conversion and control," *IEEE Trans. Energy Convers.*, vol. 35, no. 1, pp. 386–393, Mar. 2020.
[74] N. Mohan, *Advanced Electric Drives: Analysis, Control, and Modeling Using MATLAB/Simulink*. Hoboken, NJ, USA: Wiley, 2014.
[75] Y. Wang, J. Meng, X. Zhang, and L. Xu, "Control of PMSG-based wind turbines for system inertial response and power oscillation damping," *IEEE Trans. Sustain. Energy*, vol. 6, no. 2, pp. 565–574, Apr. 2015.
[76] L. Shang, J. Hu, X. Yuan, and Y. Chi, "Understanding inertial response of variable-speed wind turbines by defined internal potential vector," *Energies*, vol. 10, no. 1, p. 22, Dec. 2016.
[77] K. S. Rao and R. J. Mishra, "Comparative study of P, PI and PID controller for speed control of VSI-fed induction motor," *Int. J. Eng. Develop. Res.*, vol. 2, no. 2, pp. 2740–2744, 2014.
[78] M. Ebrahimi, S. A. Khajehoddin, and M. Karimi-Ghartemani, "An improved damping method for virtual synchronous machines," *IEEE Trans. Sustain. Energy*, vol. 10, no. 3, pp. 1491–1500, Jul. 2019.
[79] A. Ulbig, T. S. Borsche, and G. Andersson, "Impact of low rotational inertia on power system stability and operation," *IFAC Proc.*, vol. 47, no. 3, pp. 7290–7297, 2014.
[80] W. Winter, K. Elkington, G. Bareux, and J. Kostevc, "Pushing the limits: Europe's new grid: Innovative tools to combat transmission bottlenecks and reduced inertia," *IEEE Power Energy Mag.*, vol. 13, no. 1, pp. 60–74, Jan./Feb. 2015.
[81] J. Quintero, V. Vittal, G. T. Heydt, and H. Zhang, "The impact of increased penetration of converter control-based generators on power system modes of oscillation," *IEEE Trans. Power Syst.*, vol. 29, no. 5, pp. 2248–2256, Sep. 2014.
[82] Q.-C. Zhong, "Virtual synchronous machines: A unified interface for grid integration," *IEEE Power Electron. Mag.*, vol. 3, no. 4, pp. 18–27, Dec. 2016.
[83] H.-P. Beck and R. Hesse, "Virtual synchronous machine," in *Proc. 9th Int. Conf. Electr. Power Qual. Utilisation*, Oct. 2007, pp. 1–6.
[84] Q.-C. Zhong, P.-L. Nguyen, Z. Ma, and W. Sheng, "Self-synchronized synchronverters: Inverters without a dedicated synchronization unit," *IEEE Trans. Power Electron.*, vol. 29, no. 2, pp. 617–630, Feb. 2014.
[85] Q.-C. Zhong and G. Weiss, "Synchronverters: Inverters that mimic synchronous generators," *IEEE Trans. Ind. Electron.*, vol. 58, no. 4, pp. 1259–1267, Apr. 2011.
[86] S. A. Khajehoddin, M. Karimi-Ghartemani, and M. Ebrahimi, "Grid-supporting inverters with improved dynamics," *IEEE Trans. Ind. Electron.*, vol. 66, no. 5, pp. 3655–3667, May 2019.
[87] F. Gao and M. R. Iravani, "A control strategy for a distributed generation unit in grid-connected and autonomous modes of operation," *IEEE Trans. Power Del.*, vol. 23, no. 2, pp. 850–859, Apr. 2008.
[88] Y. Chen, R. Hesse, D. Turschner, and H.-P. Beck, "Improving the grid power quality using virtual synchronous machines," in *Proc. Int. Conf. Power Eng., Energy Electr. Drives*, May 2011, pp. 1–6.
[89] P. Rodriguez, I. Candela, and A. Luna, "Control of PV generation systems using the synchronous power controller," in *Proc. IEEE Energy Convers. Congr. Expo.*, Sep. 2013, pp. 993–998.
[90] Y. Chen, R. Hesse, D. Turschner, and H.-P. J. Beck, "Dynamic properties of the virtual synchronous machine (VISMA)," in *Proc. ICREPQ*, vol. 11, 2011.
[91] R. Hesse, D. Turschner, and H.-P. Beck, "Micro grid stabilization using the virtual synchronous machine (VISMA)," in *Proc. Int. Conf. Renew. Energies Power Qual. (ICREPQ)*, Valencia, Spain, 2009, pp. 15–17.
[92] S. Pulendran and J. E. Tate, "Hysteresis control of voltage source converters for synchronous machine emulation," in *Proc. 15th Int. Power Electron. Motion Control Conf. (EPE/PEMC)*, Sep. 2012, pp. LS3b.2-1–LS3b.2-8.
[93] M. P. N. van Wesenbeeck, S. W. H. de Haan, P. Varela, and K. Visscher, "Grid tied converter with virtual kinetic storage," in *Proc. IEEE Bucharest PowerTech*, Jun. 2009, pp. 1–7.
[94] S. D'Arco and J. A. Suul, "Equivalence of virtual synchronous machines and frequency-droops for converter-based microgrids," *IEEE Trans. Smart Grid*, vol. 5, no. 1, pp. 394–395, Jan. 2014.
[95] G. Delille, B. Francois, and G. Malarange, "Dynamic frequency control support by energy storage to reduce the impact of wind and solar generation on isolated power system's inertia," *IEEE Trans. Sustain. Energy*, vol. 3, no. 4, pp. 931–939, Oct. 2012.
[96] B. Zhang, X. Yan, D. Li, X. Zhang, J. Han, and X. Xiao, "Stable operation and small-signal analysis of multiple parallel DG inverters based on a virtual synchronous generator scheme," *Energies*, vol. 11, no. 1, p. 203, Jan. 2018.
[97] H. Alrajhi Alsiraji and R. El-Shatshat, "Comprehensive assessment of virtual synchronous machine based voltage source converter controllers," *IET Gener., Transmiss. Distrib.*, vol. 11, no. 7, pp. 1762–1769, May 2017.
[98] S. D'Arco and J. A. Suul, "Virtual synchronous machines—Classification of implementations and analysis of equivalence to droop controllers for microgrids," in *Proc. IEEE Grenoble Conf.*, Jun. 2013, pp. 1–7.
[99] M. Ebrahimi, S. A. Khajehoddin, and M. Karimi-Ghartemani, "An improved damping method for virtual synchronous machines," *IEEE Trans. Sustain. Energy*, vol. 10, no. 3, pp. 1491–1500, Jul. 2019.
[100] J. Morren, J. Pierik, and S. W. H. de Haan, "Inertial response of variable speed wind turbines," *Electr. Power Syst. Res.*, vol. 76, no. 11, pp. 980–987, Jul. 2006.
[101] J. Zhu, C. D. Booth, G. P. Adam, A. J. Roscoe, and C. G. Bright, "Inertia emulation control strategy for VSC-HVDC transmission systems," *IEEE Trans. Power Syst.*, vol. 28, no. 2, pp. 1277–1287, May 2013.
[102] Z. Linn, Y. Miura, and T. Ise, "Power system stabilization control by HVDC with SMES using virtual synchronous generator," *IEEJ J. Ind. Appl.*, vol. 1, no. 2, pp. 102–110, 2012.
[103] T. Shintai, Y. Miura, and T. Ise, "Reactive power control for load sharing with virtual synchronous generator control," in *Proc. 7th Int. Power Electron. Motion Control Conf.*, vol. 2, Jun. 2012, pp. 846–853.
[104] K. Visscher and S. W. H. De Haan, "Virtual synchronous machines (VSG'S) for frequency stabilisation in future grids with a significant share of decentralized generation," in *Proc. CIRED Seminar, SmartGrids Distrib.*, 2008, pp. 1–4.
[105] K. Sakimoto, Y. Miura, and T. Ise, "Stabilization of a power system with a distributed generator by a virtual synchronous generator function," in *Proc. 8th Int. Conf. Power Electron.-ECCE Asia*, 2011, pp. 1498–1505.
[106] S. D'Arco, J. A. Suul, and O. B. Fosso, "A virtual synchronous machine implementation for distributed control of power converters in SmartGrids," *Electr. Power Syst. Res.*, vol. 122, pp. 180–197, May 2015.
[107] S. D'Arco, J. A. Suul, and O. B. Fosso, "Control system tuning and stability analysis of virtual synchronous machines," in *Proc. IEEE Energy Convers. Congr. Expo.*, Jun. 2013, pp. 2664–2671.
[108] V. Kaura and V. Blasko, "Operation of a phase locked loop system under distorted utility conditions," *IEEE Trans. Ind. Appl.*, vol. 33, no. 1, pp. 58–63, Jan./Feb. 1997.

[109] H. Kolstad, "Control of an adjustable speed hydro utilizing field programmable devices," M.S. thesis, Dept. Elect. Power Eng., Norwegian Univ. Sci. Technol., Trondheim, Norway, 2002. [Online]. Available: https://www.osti.gov/etdeweb/biblio/20516841
[110] T. Inge Reigstad and K. Uhlen, "Nonlinear model predictive control of variable speed hydropower for provision of fast frequency reserves," 2020, *arXiv:2006.02097*. [Online]. Available: http://arxiv.org/abs/2006.02097
[111] D. Q. Mayne, J. B. Rawlings, C. V. Rao, and P. O. M. Scokaert, "Constrained model predictive control: Stability and optimality," *Automatica*, vol. 36, no. 6, pp. 789–814, 2000.
[112] Y. Chang, Y. Wang, F. E. Alsaadi, and G. Zong, "Adaptive fuzzy output-feedback tracking control for switched stochastic pure-feedback nonlinear systems," *Int. J. Adapt. Control*, vol. 33, no. 10, pp. 1567–1582, 2019.
[113] S. Ullah, L. Khan, R. Badar, A. Ullah, F. W. Karam, Z. A. Khan, and A. U. Rehman, "Consensus based SoC trajectory tracking control design for economic-dispatched distributed battery energy storage system," *PLoS ONE*, vol. 15, no. 5, May 2020, Art. no. e0232638.

IRFAN SAMI received the B.Sc. degree in electrical engineering from the University of Engineering and Technology Peshawar, Bannu Campus, Pakistan, in 2016, and the M.Sc. degree in electrical engineering from COMSATS University Islamabad, Abbottabad Campus, Abbottabad, Pakistan, in 2019. He is currently pursuing the Ph.D. degree in electrical engineering with Chung-Ang University, Seoul, South Korea. His research interests include electric drives, renewable energies, and electrical machine design.

NASIM ULLAH received the Ph.D. degree in mechatronics engineering from Beihang University, Beijing, China, in 2013. From 2006 to 2010, he was a Senior Design Engineer with IICS, Pakistan. He is currently an Associate Professor of Electrical Engineering with Taif University, Saudi Arabia. His research interests include renewable energy, flight control systems, integer and fractional order modeling of dynamic systems, integer/fractional order adaptive robust control methods, fuzzy/NN, hydraulic and electrical servos, epidemic, and vaccination control strategies.

S. M. MUYEEN (Senior Member, IEEE) received the B.Sc.Eng. degree in electrical and electronic engineering from the Rajshahi University of Engineering and Technology (RUET), Bangladesh, formerly known as the Rajshahi Institute of Technology, in 2000, and the M.Eng. and Ph.D. degrees in electrical and electronic engineering from the Kitami Institute of Technology, Japan, in 2005 and 2008, respectively. He is currently working as an Associate Professor with the School of Electrical Engineering Computing and Mathematical Sciences, Curtin University, Perth, WA, Australia. His research interests include power system stability and control, electrical machine, FACTS, energy storage system (ESS), renewable energy, and HVDC systems. He has been a Keynote Speaker and an Invited Speaker at many international conferences, workshops, and universities. He has published more than 225 articles in different journals and international conferences. He has published seven books, as an author or editor. He is a Fellow of Engineers Australia. He is serving as an Editor/Associate Editor for many prestigious journals from the IEEE, IET, and other publishers, including the IEEE TRANSACTIONS ON SUSTAINABLE ENERGY, the IEEE TRANSACTIONS ON ENERGY CONVERSION, the IEEE POWER ENGINEERING LETTERS, *IET Renewable Power Generation*, and *IET Generation, Transmission, and Distribution*.

KUAANAN TECHATO received the B.Eng. (ME) degree from the Prince of Songkla University, Thailand, in 1995, the M.Eng. (IE) degree from Chulalongkorn University, in 1999, the M.Sc. (EBM) degree from Warwick University, in 1999, and the Ph.D. degree from Chulalongkorn University, in 2008. He is currently working as an Assistant Professor with the Prince of Songkla University, Hadyai Campus, Thailand, where he is also serving as the Dean for the Faculty of Environmental Management. His research interests include renewable energy, heat-pump, power systems, and control. He has been a Keynote Speaker and an Invited Speaker at many international conferences. He has published many technical articles to various journals and international conferences. He is also involved with many journals, as an Editor or Associate Editor and a Successful Organizer for many international conferences.

MD. SHAHARIAR CHOWDHURY received the B.Sc. degree in engineering (EEE) from the Atish Dipankar University Science Technology, Bangladesh, in 2015, the M.Sc. degree from the Prince of Songkla University, in 2019, and the M.Sc. degree from Universiti Kebangsaan Malaysia (UKM), in 2019. He is currently working as a Research Fellow with the Prince of Songkla University, Hatyai, Thailand. His research interests include renewable energy, solar PV, thin film, perovskite solar cells, solar PV waste recycling, and semiconductor materials. He has published a review article and research article in the ISI index journal. His research area highlighted twice in the sustainable newspaper (Eco-business.com). He is an Editorial Member of the *International Journal of Sustainable and Renewable Energy*.

JONG-SUK RO received the B.S. degree in mechanical engineering from Han-Yang University, Seoul, South Korea, in 2001, and the Ph.D. degree in electrical engineering from Seoul National University (SNU), Seoul, in 2008. He conducted research at the Research and Development Center, Samsung Electronics, as a Senior Engineer, from 2008 to 2012. From 2012 to 2013, he was with the Brain Korea 21 Information Technology of SNU, as a Postdoctoral Fellow. From 2013 to 2016, he worked with the Brain Korea 21 Plus, SNU, as a B. K. Assistant Professor. He conducted research at the Electrical Energy Conversion Systems Research Division, Korea Electrical Engineering and Science Research Institute, as a Researcher, in 2013. In 2014, he was with the University of Bath, Bath, U.K., as an Academic Visitor. He is currently an Associate Professor with the School of Electrical and Electronics Engineering, Chung-Ang University, Seoul. His research interests include the analysis and optimal design of next-generation electrical machines using smart materials, such as electromag- nets, piezoelectric, and magnetic shape memory alloys.